Phytochemistry 176 (2020) 112415

Contents lists available at ScienceDirect

Phytochemistry

journal homepage: www.elsevier.com/locate/phytochem

Bufadienolide glycosides and bufadienolides from the whole plants of *Helleborus lividus*, and their cytotoxic activity

Tomoki Iguchi, Akihito Yokosuka*, Naoya Tamura, Shingo Takano, Yoshihiro Mimaki

Department of Medicinal Pharmacognosy, School of Pharmacy, Tokyo University of Pharmacy and Life Sciences, 1432-1 Horinouchi, Hachioji, Tokyo, 192-0392, Japan

ARTICLE INFO

Keywords:
Helleborus lividus
Ranunculaceae
Bufadienolides
Bufadienolide glycosides
Cytotoxicity
Apoptosis
HL-60 cells
A549 cells
Na^+/K^+ ATPase

ABSTRACT

Cytotoxicity-guided fractionation of the MeOH extract of *Helleborus lividus* Aiton ex Curtis (Ranunculaceae) resulted in the isolation of five undescribed bufadienolide glycosides and two undescribed bufadienolides, along with three known compounds. Their structures were determined by detailed spectroscopic analysis and hydrolysis studies. The isolated compounds showed cytotoxicity against HL-60 human leukemia cells and A549 human lung adenocarcinoma cells, with IC_{50} values ranging from 2.20 ± 0.01 nM to 0.77 ± 0.01 μM. The undescribed compound 3β-[(*O*-β-D-glucopyranosyl-(1 → 4)-α-L-rhamnopyranosyl)oxy]-14β,16β-dihydroxy-5β-bufa-20,22-dienolide induced apoptosis in HL-60 cells via a mitochondria-dependent apoptotic pathway. The average IC_{50} values of bufadienolide monorhamnosides for HL-60 and A549 cells were 10–20 times lower than those for Na^+/K^+ ATPase, implying that they induce tumor cell death via a mechanism of action other than Na^+/K^+ ATPase inhibition.

1. Introduction

The genus *Helleborus*, belonging to the Ranunculaceae family, has about 20 different species, most of which are cultivated for an ornamental purpose (Tsukamoto, 1989). *Helleborus* species have been reported to contain steroidal components, such as bufadienolides and ecdysteroids (Cheng et al., 2014; Meng et al., 2001; Zhang et al., 2014). Previously, we have investigated the chemical constituents of the rhizomes of *Helleborus orientalis* Lam. and the whole plants of *Helleborus foetidus* L., and successfully isolated structurally diverse steroidal compounds (Iguchi et al., 2020; Yokosuka et al., 2018; Watanabe et al., 2003). *Helleborus lividus* Aiton ex Curtis is native to the Majorca islands in Spain. To date, neither a phytochemical study nor a biological activity evaluation of the plant has been conducted. Since the MeOH extract of *H. lividus* whole plants exhibited cytotoxic activity against HL-60 human leukemia cells, we conducted a phytochemical study of the extract as a part of our ongoing study of cytotoxic constituents derived from Ranunculaceae plants. Five previously undescribed bufadienolide glycosides (**1**–**3**, **6**, and **7**), and two bufadienolides (**4** and **5**), along with three known compounds (**8**–**10**), were isolated. Herein, we report the isolation and structural determination of the isolated compounds (**1**–**10**) and their cytotoxic activities against HL-60 human leukemia cells, A549 human lung adenocarcinoma cells, and TIG-3 human normal diploid lung cells. The apoptosis-inducing activity of the bufadienolide diglycoside **7** and Na^+/K^+ ATPase inhibitory activity of the isolated compounds are also described.

2. Results and discussion

The whole plants of *H. lividus* were extracted with hot MeOH. The MeOH extract, which showed cytotoxicity against HL-60 cells with an IC_{50} value of 1.3 μg/mL, was passed through a porous-polymer polystyrene resin (Diaion HP-20) column, and was successively eluted with MeOH–H_2O mixtures, MeOH, EtOH, and EtOAc. The portions eluted with 50% aqueous MeOH and 100% MeOH eluted were cytotoxic to HL-60 cells with IC_{50} values of 0.15 μg/mL and 0.16 μg/mL, respectively, and were subjected to multiple chromatographic steps over silica (Si) gel and octadecylsilanized (ODS) Si gel, as well as to preparative HPLC to yield compounds **1**–**10**. Their structures were determined by spectroscopic analysis of the UV, IR, 1D and 2D (COSY, HSQC, HMBC, and NOESY) NMR spectra, and mass spectrometry, as well as comparison of their spectroscopic data with those reported previously.

Based on comparison of the physical and spectroscopic data of **8**–**10** with those reported in the literature, **8**–**10** were identified as 16β-hydroxyhellebrigenin (**8**) (Krenn et al., 2000) and 16β-hydroxyhellebrigenin 3-*O*-β-D-glucopyranoside (**9**), (Krenn et al., 2000), and 5β,14β-dihydroxy-19-oxo-3β-[(α-L-rhamonopyranosyl)oxy]-bufa-20,22-dienolide (**10**) (Watanabe et al., 2003) (Fig. 1), which were

* Corresponding author.
E-mail address: yokosuka@toyaku.ac.jp (A. Yokosuka).

https://doi.org/10.1016/j.phytochem.2020.112415
Received 7 January 2020; Received in revised form 13 May 2020; Accepted 15 May 2020

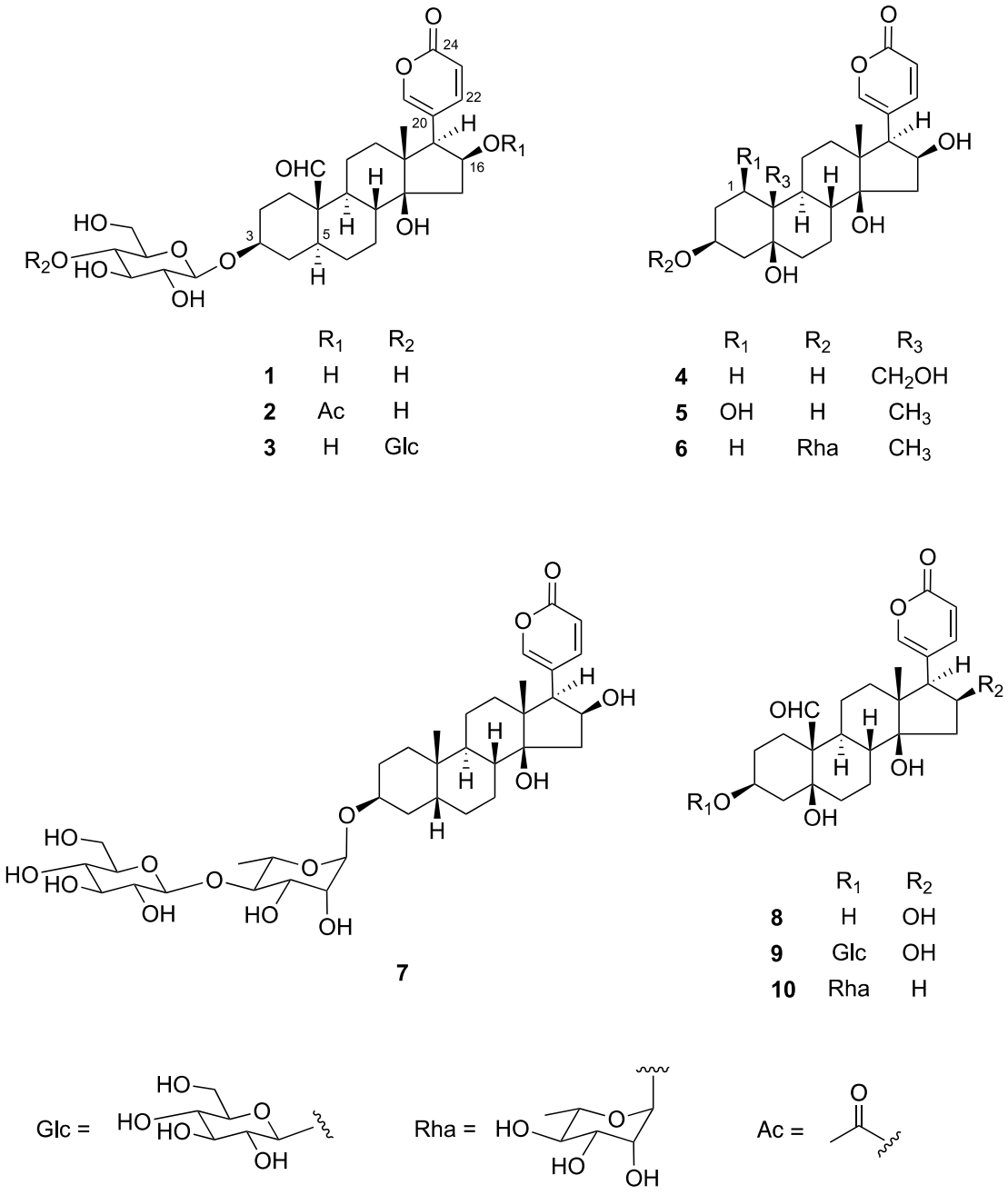

Fig. 1. Structures of **1**–**10**.

previously isolated from *Urginea maritima* (Asparagaceae) (**8** and **9**) and *Helleborus orientalis* (Ranunculaceae) (**10**), respectively.

Compound **1** was obtained as an amorphous solid with a molecular formula of $C_{30}H_{42}O_{11}$ as determined by HRESITOFMS (*m/z* 601.2620 $[M + Na]^+$, calcd for $C_{30}H_{42}NaO_{11}$: 601.2625) and ^{13}C NMR spectral data. The IR spectrum of **1** suggested the presence of hydroxy (3397 cm^{-1}) and carbonyl groups (1706 and 1695 cm^{-1}). The UV spectrum showed absorption maxima indicative of a conjugated system (295 and 204 nm). The ^1H and ^{13}C NMR spectra of **1** contained signals attributable to a 2-pyrone ring moiety [δ_H 8.10 (dd, J = 9.7, 2.4 Hz, H-22), 7.42 (dd, J = 2.4, 0.8 Hz, H-21), 6.18 (dd, J = 9.7, 0.8 Hz, H-23)/δ_C 120.3, 151.8, 152.8, 112.9, and 165.0 (C-20–C-24)], which was characteristic of the bufadienolide structure, a methyl group [δ_H 0.71 (s, H_3-18)/δ_C 17.1 (C-18)], an aldehyde group [δ_H 9.99 (s, H-19)/δ_C 210.4 (C-19)], two oxymethine groups [δ_H 4.46 (br dd, J = 7.9, 7.7 Hz, H-16)/δ_C 73.2 (C-16); 3.75 (m, $W_{1/2}$ = 19.4 Hz, H-3)/δ_C 78.5 (C-3)], a quaternary carbon with an oxygen atom [δ_C 85.3 (C-14)], two quaternary carbon atoms [δ_C 52.8 (C-10), 50.1 (C-13)], and an anomeric proton/carbon [δ_H 4.37 (d, J = 7.8 Hz, H-1′)/δ_C 102.4 (C-1′)] (Tables 1 and 2). Enzymatic hydrolysis of **1** with naringinase gave 16β-hydroxybovogenin (3β,14β,16β-trihydroxy-19-oxo-5α-bufa-20,22-dienolide: **1a**) (Van Wyk and Enslin, 1968) as the aglycone, and D-glucose (Glc) as the carbohydrate moiety. The structure of **1a** was identified by analysis of the 1D and 2D NMR spectra. The A/B *trans*, B/C *trans*, and C/D *cis* ring junctions, and the 14β and 16β configurations were determined by NOE correlations in the NOESY spectrum. The identification of D-glucose, including its absolute configuration, was carried out by direct HPLC analysis of the hydrolysate, using an optical rotation detector. In the HMBC spectrum of **1**, a long-range correlation was observed between H-1' of Glc at δ_H 4.37 and C-3 of the aglycone at δ_C 78.5 (Fig. 2). The anomeric configuration of the Glc moiety was determined to be the β-form by the relatively large $^3J_{H\text{-}1,H\text{-}2}$ value (7.8 Hz) in the ^1H NMR

Table 1
^{1}H NMR chemical shift assignments of **1–7** in CD_3OD.[a)]

Position	1	2	3	4	5	6	7
1 a	2.41 m	2.42 m	2.43 m	2.34 m	3.92 br s	1.73 m	1.54 m
b	1.02 m	1.05 m	1.03 m	1.43 m		1.47 m	1.41 m
2 a	1.97 m	2.00 m	1.99 m	1.76 m	2.04 m	1.73 m	1.64 m
b	1.31 m	1.32 m	1.30 m	1.70 m	2.04 m	1.69 m	1.58 m
3	3.75 m (19.4)[b)]	3.77 m (15.7)[b)]	3.75 m (15.7)[b)]	4.10 br s	4.23 br s	4.16 br s	3.95 br s
4 a	1.94 m	1.93 m	1.93 m	2.23 m	2.35 m	2.22 m	1.88 m
b	1.27 m	1.30 m	1.29 m	1.43 m	1.70 m	1.64 m	1.47 m
5	1.41 m	1.42 m	1.42 m	–	–	–	1.65 m
6 a	2.00 m	2.03 m	2.03 m	1.91 m	1.73 m	1.75 m	1.87m
b	1.59 m	1.63 m	1.62 m	1.51 m	1.36 m	1.36 m	1.28 m
7 a	2.28 m	2.28 m	2.30 m	2.04 m	2.04 m	2.02 m	1.91 m
b	1.22 m	1.29 m	1.28 m	1.25 m	1.26 m	1.23 m	1.26 m
8	1.58 m	1.60 m	1.60 m	1.70 m	1.43 m	1.63 m	1.60 m
9	1.23 m	1.30 m	1.25 m	1.69 m	1.66 m	1.60 m	1.69 m
10	–	–	–	–	–	–	–
11	1.69 m	1.73 m	1.71 m	1.51 m	1.36 m	1.45 m	1.44 m
	1.19 m	1.20 m	1.21 m	1.25 m	1.36 m	1.27 m	1.21 m
12	1.56 m	1.55 m	1.54 m	1.57 m	1.54 m	1.57 m	1.57 m
	1.28 m	1.35 m	1.29 m	1.31 m	1.33 m	1.38 m	1.38 m
13	–	–	–	–	–	–	–
14	–	–	–	–	–	–	–
15	2.44 dd (14.9, 7.7)	2.59 dd (15.5, 8.5)	2.45 dd (14.9, 7.7)	2.50 dd (14.8, 7.7)	2.49 dd (14.8, 7.7)	2.53 dd (14.8, 7.7)	2.55 dd (14.8, 7.6)
	1.71 br d (14.9)	1.80 br d (15.5)	1.74 br d (14.9)	1.76 br d (14.8)	1.77 br d (14.8)	1.77 br d (14.8)	1.78 br d (14.8)
16	4.46 br dd (7.9, 7.7)	5.47 br t (8.5, 8.5)	4.48 br dd (7.9, 7.7)	4.50 br dd (7.9, 7.7)	4.49 br dd (7.9, 7.7)	4.50 br dd (7.9, 7.7)	4.50 br dd (7.9, 7.6)
17	2.72 d (7.9)	2.95 d (8.5)	2.74 d (7.9)	2.75 d (7.9)	2.74 d (7.9)	2.77 d (7.9)	2.75 d (7.9)
18	0.71 s	0.72 s	0.71 s	0.77 s	0.79 s	0.78 s	0.78 s
19	9.99 s	9.99 s	9.99 s	4.23 d (11.4)	1.19 s	0.94 s	0.94 s
				3.55 d (11.4)			
20	–	–	–	–	–	–	–
21	7.42 dd (2.4, 0.8)	7.42 br s	7.43 dd (2.5, 0.7)	7.43 br d(2.4)	7.43 dd (2.5, 0.8)	7.45 dd (2.4, 0.8)	7.44 dd (2.5, 0.8)
22	8.10 dd (9.7, 2.4)	8.22 br d (9.8)	8.11 dd (9.8, 2.5)	8.11 dd (9.7, 2.4)	8.11 dd (9.7, 2.5)	8.13 dd (9.8, 2.4)	8.11 dd(9.7, 2.5)
23	6.18 dd (9.7, 0.8)	6.20 br d (9.8)	6.18 dd (9.8, 0.7)	6.18 br d (9.7)	6.18 dd (9.7, 0.8)	6.19 dd (9.8, 0.8)	6.18 dd (9.7, 0.8)
24	–	–	–	–	–	–	–
Ac 16-$OCOCH_3$		1.84 s					
1'	4.37 d (7.8)	4.38 d (8.1)	4.41 d (7.8)			4.85 d (1.6)	4.76 br s
2'	3.11 dd (9.1,7.8)	3.12 dd (8.9, 8.1)	3.12 dd (8.9, 7.8)			3.78 dd (3.4, 1.6)	3.78 br d (3.3)
3'	3.33 m	3.33 m	3.50 dd (8.9, 8.9)			3.63 m	3.91 dd (9.4, 3.3)
4'	3.24 m	3.26 m	3.54 dd (8.9, 8.9)			3.40 dd (9.5, 9.5)	3.61 dd (9.4, 9.4)
5'	3.25 m	3.25 m	3.40 m			3.64 m	3.70 m
6' a	3.84 dd (11.3, 1.1)	3.85 dd (11.3, 1.1)	3.85 m			1.25 d (6.2)	1.31 d (6.2)
b	3.63 m	3.64 m	3.66 m				
1"			4.39 d (7.9)				4.58 d (7.8)
2"			3.22 dd (8.9, 7.9)				3.21 dd (8.6, 7.8)
3"			3.37 m				3.37 m
4"			3.32 m				3.30 m
5"			3.34 m				3.27 m
6" a			3.84 m				3.84 m
b			3.65 m				3.69 m

[a] 500 MHz for **1**, **5** and **7**. 600 MHz for **2–4** and **6**.
[b] $W_{1/2}$.

spectrum. Therefore, the structure of **1** was elucidated to be 3β-[(β-D-glucopyranosyl)oxy]-14β,16β-dihydroxy-19-oxo-5α-bufa-20,22-dienolide.

Compound **2** ($C_{32}H_{44}O_{12}$) was obtained as an amorphous solid. The spectral features of **2** revealed that it was a bufadienolide glucoside closely related to **1**. The presence of an acetyl group in **2** was indicated in the ^{1}H and ^{13}C NMR spectra [δ_H 1.84 (s)/δ_C 171.9 (C=O) and 20.8 ($\underline{C}H_3$)]. Alkaline treatment of **2** with 0.5% NaOMe in MeOH gave **1**, indicating that **2** must be a monoacetate of **1**. The ester linkage at C-16 of the aglycone was evident from a long-range correlation between H-16 of the aglycone at δ_H 5.47 (br dd, J = 8.5, 8.5 Hz) and the acetyl carbonyl carbon at δ_C 171.9 in the HMBC spectrum of **2**. Therefore, the structure of **2** was elucidated to be 16β-acetoxy-3β-[(β-D-glucopyranosyl)oxy]-14β-hydroxy-19-oxo-5α-bufa-20,22-dienolide.

Compound **3** was also a bufadienolide glucoside based on its spectral features, and its molecular formula was determined to be $C_{36}H_{32}O_{16}$ based on HESITOFMS (m/z: 763.3156 [M + Na]$^+$) and ^{13}C NMR data. The deduced molecular formula was higher than that of **1** by $C_6H_{10}O_5$. Enzymatic hydrolysis of **3** under the same conditions as **1** resulted in the production of **1a** and D-glucose, suggesting that **3** was a diglucoside of **1a**. Analysis of the ^{1}H–^{1}H COSY and HSQC spectra of **3** indicated that the sugar moiety of **3** was composed of a β-D-glucopyranosyl moiety (Glc-II) [δ_H 4.39 (d, J = 7.9 Hz) (H-1'')]; δ_C 104.6, 74.9, 77.9, 71.4, 78.1, 62.4] and a 4-substituted β-D-glucopyranosyl moiety (Glc-I) [δ_H 4.41 (d, J = 7.8 Hz) (H-1′); δ_C 102.3, 74.8, 76.4, 80.7, 76.4, 61.9]. The HMBC spectrum showed correlation peaks between H-1'' of Glc-II at δ_H 4.39 and C-4 of Glc at δ_C 80.7 and between H-1' of Glc-I at δ_H 4.41 and C-3 of the aglycone at δ_C 78.6. Thus, the structure of **3** was determined to be 3β-[(*O*-β-D-glucopyranosyl-(1 → 4)-β-D-glucopyranosyl)oxy]-14β,16β-dihydroxy-19-oxo-5α-bufa-20,22-dienolide.

Compound **4** ($C_{24}H_{34}O_7$) was obtained as an amorphous solid. The ^{1}H NMR spectrum of **4** contained signals attributable to a 2-pyrone ring [δ_H 8.11 (dd, J = 9.7, 2.4 Hz, H-22), 7.43 (br d, J = 2.4 Hz, H-21), 6.18 (1H, br d, J = 9.7 Hz, H-23)], two oxymethine protons [δ_H 4.10 (br s, H-3) and 4.50 (br dd, J = 7.9, 7.7 Hz, H-16)], and a pair of hydroxymethyl protons [δ_H 4.23 (d, J = 11.4 Hz, H-19a) and 3.55 (d, J = 11.4 Hz, H-19b)]. The ^{13}C NMR spectrum of **4** displayed signals assignable to two oxymethine carbons [δ_C 68.8 (C-3) and 73.3 (C-16)],

Table-2
^{13}C NMR data of **1–7** in CD_3OD.[a)]

	1	2	3	4	5	6	7
1	32.1	32.2	32.1	20.1	74.7	26.7	31.6
2	31.6	31.6	31.5	28.2	34.5	26.8	27.5
3	78.5	78.5	78.6	68.8	68.5	76.1	73.9
4	36.8	36.8	36.8	38.0	39.1	35.4	30.9
5	44.0	44.0	44.0	78.7	76.1	75.7	38.2
6	29.6	29.5	29.6	36.8	36.5	35.6	22.6
7	28.7	28.4	28.7	25.0	24.8	24.8	27.9
8	44.1	44.2	44.1	41.8	42.2	41.9	43.0
9	[b)]	49.8	49.6	40.0	42.1	40.1	36.9
10	52.8	52.7	52.8	43.6	44.5	41.8	36.3
11	22.9	22.9	22.9	22.7	22.6	22.7	22.4
12	41.5	40.8	41.5	42.3	41.7	42.0	42.0
13	50.1	50.5	50.1	50.2	50.2	50.2	50.4
14	85.3	84.4	85.3	85.9	85.6	85.8	86.0
15	42.6	40.6	42.5	42.9	43.1	43.2	43.1
16	73.2	75.5	73.2	73.3	73.2	73.3	73.4
17	59.4	58.1	59.3	59.4	59.3	59.4	60.0
18	17.1	16.9	17.1	17.2	17.2	17.2	17.3
19	210.4	210.4	210.4	65.9	13.2	17.3	22.4
20	120.3	119.2	120.3	120.4	120.4	120.4	120.5
21	151.8	152.9	151.8	151.8	151.8	151.8	151.7
22	152.8	152.0	152.8	152.8	152.8	152.9	152.9
23	112.9	113.2	112.9	112.9	112.9	112.9	112.9
24	165.0	164.4	165.0	165.0	165.0	165.1	165.1
1'	102.4	102.3	102.3			101.0	99.8
2′	75.1	75.1	74.8			72.6	72.8
3′	78.1	78.1	76.4			72.5	72.6
4′	71.1	71.8	80.7			73.8	83.6
5′	77.9	77.9	76.4			70.7	68.7
6′	62.8	62.9	61.9			17.9	18.1
1"			104.6				105.8
2"			74.9				76.1
3"			77.9				78.2
4"			71.4				71.5
5"			78.1				78.1
6"			62.4				62.7
Ac		20.8					
		171.9					

[a] 125 MHz for **1**, **5** and **7**, 150 MHz for **2–4** and **6**.
[b] Signal is unclear due to overlapping with solvent signals.

a hydroxymethyl carbon [δ_C 65.9 (C-19)], and two quaternary carbons bearing oxygen atoms [δ_C 78.7 (C-5) and 85.9 (C-14)]. These data implied that **4** was a bufadienolide derivative with five hydroxy groups. The ^{1}H and ^{13}C NMR spectral data of **4** were closely related to those of 16β-hydroxyhellebrigenin (3β,5β,14β,16β-tetrahydroxy-19-oxobufa-20,22-dienolide: **8**); however, the ^{1}H and ^{13}C NMR signals corresponding to the C-19 aldehyde group [δ_H 10.5 (s)/δ_C 209.0] in **8** were replaced by the signals due to the hydroxymethyl proton and carbon [δ_H 4.23 (d, J = 11.4 Hz) and 3.55 (d, J = 11.4 Hz)/δ_C 65.9] in **4**. In the HMBC spectrum of **4**, long-range correlations were observed from δ_H 4.23 (H-19a) and 3.55 (H-19b) to δ_C 20.1 (C-1), 78.7 (C-5), 40.0 (C-9), and 43.6 (C-10) (Fig. 2). Therefore, **4** was deduced to have hydroxy groups at C-3, C-5, C-14, C-16, and C-19. The A/B *cis*, B/C *trans*, and C/D *cis* ring fusions of the bufadienolide skeleton and the C-3β, C-5β, C-14β, C-16β, and C-17β configurations were elucidated based on the NOE correlations in the NOESY spectrum of **4** (Fig. 3). Altogether, the structure of **4** was elucidated to be 3β,5β,14β,16β,19-pentahydroxybufa-20,22-dienolide.

The ^{1}H and ^{13}C NMR spectral data of **5** ($C_{24}H_{34}O_7$) were similar to those of **4**; however, **5** differed from **4** in terms of the signals arising from the A and B ring portions (C-1–10 and C-19). Instead of the signals for the C-1 methylene and the C-19 hydroxymethyl protons and carbons [δ_H 2.34 (m, H-1a) and 1.43 (m, H-1b)/δ_C 65.9 (C-1); δ_H 4.23 (d, J = 11.4 Hz, H-19a) and 3.55 (d, J = 11.4 Hz, H-19b)/δ_C 65.9 (C-19)], signals assignable to an oxymethine group [δ_H 3.92 (br s, H-1)/δ_C 74.7 (C-1)] and an angular methyl group [δ_H 1.19 (s, Me-19)/δ_C 13.2 (C-19)] were observed in **5**. All other ^{1}H and ^{13}C signals appeared at almost the same positions for the two compounds. The configurations of the hydroxy groups were ascertained to be C-1β, C-3β, C-5β, C-14β, and C-16β, respectively, based on the NOE correlations in the NOESY spectrum of **5** (Fig. 3). Thus, the structure of **5** was established as 1β,3β,5β,14β,16β-pentahydroxybufa-20,22-dienolide.

The ^{1}H and ^{13}C NMR spectral features of **6** ($C_{30}H_{44}O_{10}$) were analogous to those of **5**. However, the H-1/C-1 hydroxymethine signals [δ_H 3.92 (br s)/δ_C 74.7] in **5** were substituted by the methylene signals [δ_H 1.73 (m, H-1a) and 1.47 (m, H-1b)/δ_C 26.7 (C-1)] in **6**. Furthermore, signals for an α-L-rhamnopyranosyl moiety (Rha) were observed in the ^{1}H and ^{13}C NMR spectra of **6** [δ_H 4.85 (1H, d, J = 1.6 Hz); δ_C 101.0, 72.6, 72.5, 73.8, 70.7, 17.9 (C-1′–C-6′)]. Acid hydrolysis of **6** gave L-rhamnose, whereas the aglycone decomposed under acidic conditions. The HMBC spectrum of **6** exhibited a correlation between H-1′ of Rha at δ_H 4.85 and C-3 of the aglycone at δ_C 76.1. The anomeric proton of the L-rhamnosyl moiety was equatorial, and therefore possessed an α-pyranoid anomeric form (^{1}C$_4$) due to the large.

$^1J_{C\text{-}1,H\text{-}1}$ value (174.2 Hz) in the proton-coupled ^{13}C NMR spectrum (Bock et al., 1973). Thus, the structure of **6** was determined to be 5β,14β,16β-trihydroxy-3β-[(α-L-rhamnopyranosyl)oxy]-bufa-20,22-dienolide.

Compound **7** ($C_{36}H_{54}O_{14}$) also showed spectral features that are characteristic of a bufadienolide glycoside. Enzymatic hydrolysis of **7** with naringinase gave desacetylbufotalin (3β,14β,16β-trihydroxy-5β-bufa-20,22-dienolide: **7a**) (Verpoorte et al., 1980), D-glucose (Glc), and L-rhamnose (Rha). A combination of ^{1}H–^{1}H COSY and HSQC spectral analyses indicated that the sugar moiety of **7** comprised a β-D-glucopyranosyl moiety (Glc) [δ_H 4.58 (1H, d, J = 7.8 Hz); δ_C 105.8, 76.1, 78.2, 71.5, 78.1, 62.7] and a 4-substituted α-L-rhamnopyranosyl moiety (Rha) [δ_H 4.76 (1H, br s); δ_C 99.8, 72.8, 72.6, 83.6, 68.7, 18.1]. The HMBC spectrum showed correlation peaks between H-1" of Glc at δ_H 4.58 and C-4 of Rha at δ_C 83.6, and between H-1' of Rha at δ_H 4.76 and C-3 of the aglycone at δ_C 73.9. The configuration of the anomeric proton of the L-rhamnose moiety was deduced to be α besed on the large $^1J_{C\text{-}1,H\text{-}1}$ value (167.4 Hz), and that of the D-glucose moiety was deduced to be β based on the relatively large $^3J_{H\text{-}1,H\text{-}2}$ value (7.8 Hz). Thus, the structure of **7** was elucidated to be 3β-[(*O*-β-D-glucopyranosyl-(1 → 4)-α-L-rhamnopyranosyl)oxy]-14β,16β-dihydroxy-5β-bufa-20,22-dienolide.

Compounds **1–10** were evaluated for their cytotoxic activity against HL-60 and A549 tumor cells, as well as TIG-3 normal cells, using a modified MTT assay. Although **1–10** did not show tumor-selective cytotoxicity, **1–3** and **6–10** were considerably more cytotoxic to both HL-60 and A549 cells than the positive controls, etoposide, cisplatin, and doxorubicin, with IC_{50} values ranging from 0.0022 to 0.085 μM (Table 3). Compound **2** was a 16-*O*-acetyl derivative of **1** and its cytotoxicity to HL-60 and A549 cells (IC_{50} 0.015 ± 0.001 μM for HL-60 cells; IC_{50} 0.0086 ± 0.0003 μM for A549 cells) was more potent than that of **1** (IC_{50} 0.085 ± 0.003 μM for HL-60 cells; IC_{50} 0.026 ± 0.002 μM for A549 cells). The hydroxymethyl group at C-19 in **4** was substituted by an aldehyde group in **8**, and the cytotoxic activity of **8** (IC_{50} 0.040 ± 0.001 μM for HL-60 cells; IC_{50} 0.0120 ± 0.0003 μM for A549 cells) was found to be more potent than that of **4** (IC_{50} 0.110 ± 0.001 μM for HL-60 cells; IC_{50} 0.130 ± 0.003 μM for A549 cells).

Compound **7** was a previously undescribed bufadienolide diglycoside and showed potent cytotoxicity against HL-60 and A549 cells with IC_{50} values of 0.021 ± 0.001 and 0.018 ± 0.001 μM, respectively. Then, the apoptosis-inducing activity of **7** was evaluated in HL-60 cells. Morphological characteristics of condensed and fragmented nuclei, induction of DNA fragmentation, and caspase-3 activation were observed in HL-60 cells treated with **7** (Fig. 4). Disruption of the mitochondrial membrane potential and release of cytochrome *c* from mitochondria into the cytoplasm were also observed in **7**-treated HL-60 cells (Fig. 5). These data implied that **7** induced apoptosis through a mitochondria-dependent pathway in HL-60 cells.

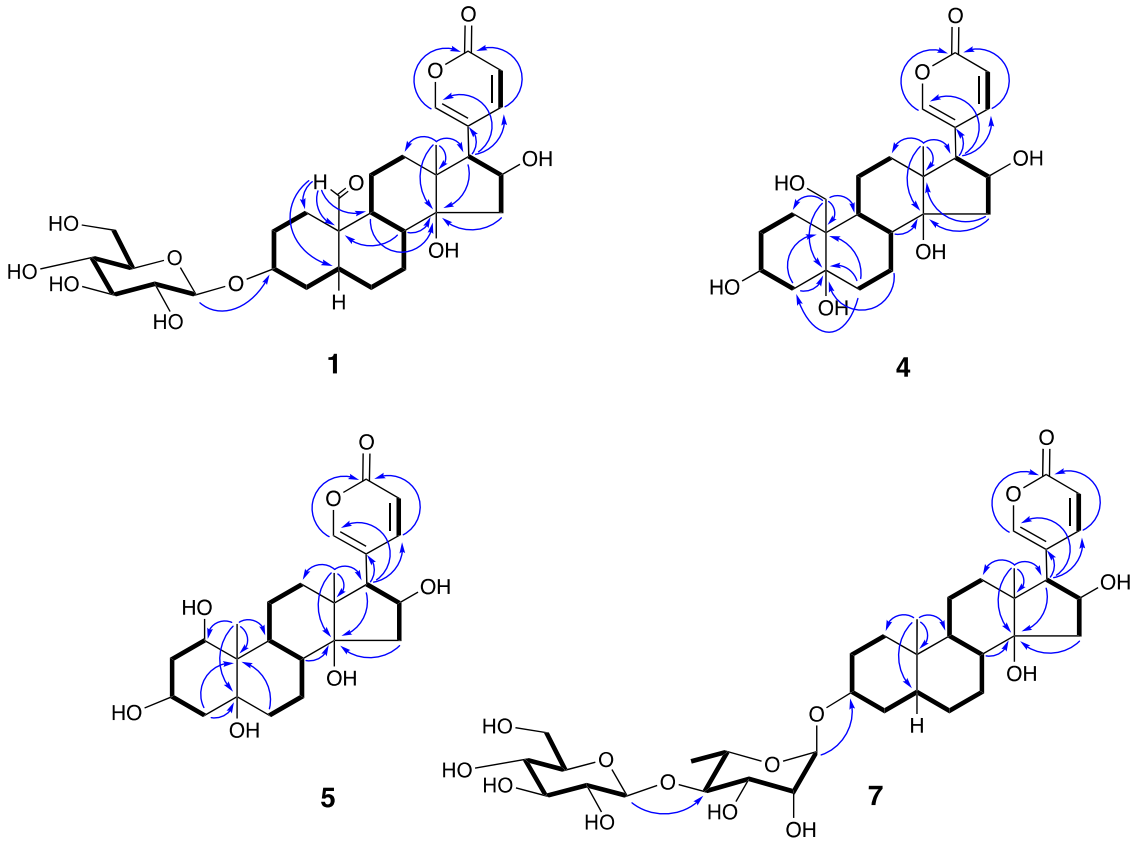

Fig. 2. Key HMBC correlations of **1**, **4**, **5** and **7**.
Bold lines indicate the ^{1}H–^{1}H coupling, and arrows indicate $^{1}H/^{13}C$ long-range correlations.

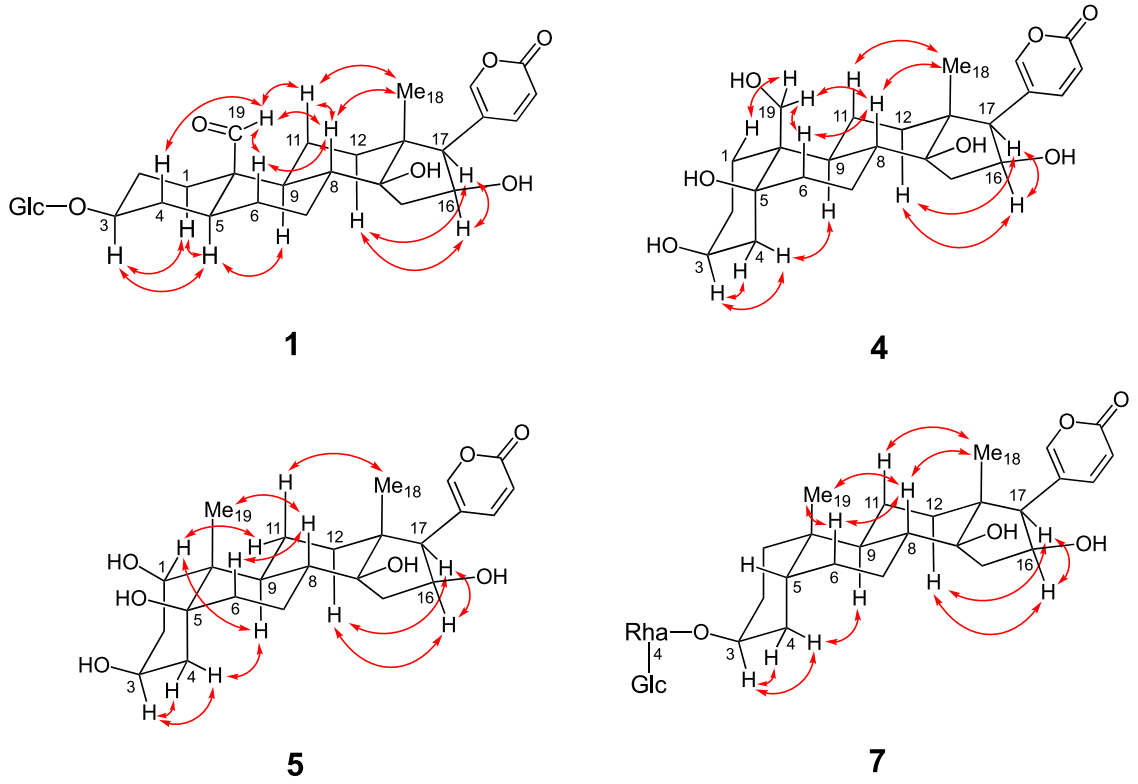

Fig. 3. Key NOE correlations of **1**, **4**, **5** and **7**.

Table 3
Cytotoxicity of the isolated compounds **1**–**10**, etoposide, cisplatin, and doxorubicin against HL-60, A549, and TIG-3 cells.

Compounds	IC_{50} (μM)		
	HL-60	A549	TIG-3
1	0.085 ± 0.003	0.026 ± 0.002	0.0150 ± 0.0004
2	0.015 ± 0.001	0.0086 ± 0.0003	0.0051 ± 0.0001
3	0.065 ± 0.001	0.034 ± 0.002	0.014 ± 0.001
4	0.110 ± 0.001	0.130 ± 0.003	0.0130 ± 0.0003
5	0.770 ± 0.012	0.420 ± 0.019	0.190 ± 0.009
6	0.0250 ± 0.0003	0.0230 ± 0.0004	0.012 ± 0.001
7	0.021 ± 0.001	0.018 ± 0.001	0.0096 ± 0.0001
8	0.040 ± 0.001	0.0120 ± 0.0003	0.0055 ± 0.0002
9	0.0094 ± 0.0003	0.0096 ± 0.0002	0.0036 ± 0.0001
10	0.0023 ± 0.0001	0.0022 ± 0.0001	0.00093 ± 0.00001
etoposide	0.180 ± 0.001	–[a]	–
cisplatin	1.10 ± 0.02	2.30 ± 0.39	1.70 ± 0.02
doxorubicin	–	0.17 ± 0.02	0.60 ± 0.03

[a] Not determined.

Bufadienolides are classified as cardiotonic steroids, and have been reported to inhibit Na^+/K^+ ATPase, which resulted in increased intracellular Ca^{2+} concentrations followed by tumor cell death, including the induction of apoptotic cell death (Zeino et al., 2015). Then, the Na^+/K^+ ATPase inhibitory activities of the isolated compounds (**1**–**10**) were evaluated (Table 4). Compounds **1**–**5** and **7**–**9** inhibited Na^+/K^+ ATPase with IC_{50} values ranging from 0.037 to 0.45 μM, suggesting that their cytotoxicity was partially mediated via the inhibition of Na^+/K^+ ATPase. On the other hand, the average IC_{50} values of bufadienolide monorhamnosides (**6** and **10**) for HL-60 and A549 cells were 10–20 times lower than those for Na^+/K^+ ATPase, which imply that **6** and **10** induce tumor cell deaths via a pathway not involving Na^+/K^+ ATPase inhibition.

3. Conclusions

The whole plants of *H. lividus* yielded five bufadienolide glycosides (**1**–**3**, **6**, and **7**) and two bufadienolides (**4** and **5**), along with three already known compounds (**8**–**10**) upon MeOH extraction. More than 700 bufadienolide derivatives, which were reported until now, contained A/B *cis* (5β) steroid ring fusion, whereas **1**–**3** with A/B *trans* (5α) ring fusion are a unique type of bufadienolide derivatives, which rarely occurred in the plant kingdom. Compounds **1**–**10** exhibited potent cytotoxicity to both HL-60 and A549 cells. Compound **7** induced cell death in HL-60 cells via a mitochondrial-dependent apoptotic pathway. The average IC_{50} values of bufadienolide monorhamnosides (**6** and **10**) for HL-60 and A549 cells were 10–20 times lower than those for Na^+/K^+ ATPase, implying that they induce tumor cell deaths via a pathway not involving Na^+/K^+ ATPase inhibition.

4. Experimental

4.1. General experimental procedures

Optical rotations were measured by using a JASCO P-1030 (Tokyo, Japan) automatic digital polarimeter. UV spectra were measured with a JASCO V-630 UV–Vis spectrophotometer (Tokyo, Japan). IR spectra were recorded on a JASCO FT-IR 620 spectrophotometer. NMR spectral data were obtained on a DRX-600 (600 MHz for ^{1}H-NMR, Bruker, Karlsruhe, Germany) for **2**–**4** and **6**, and DRX-500 spectrometer (500 MHz for ^{1}H-NMR, Bruker) for **1**, **5** and **7**, using standard Bruker pulse programs at 300 K. Chemical shifts were given as δ values with reference to tetramethylsilane (TMS) as an internal standard. ESITOFMS data were recorded on an LCT mass spectrometer (Waters-Micromass, Manchester, UK). Porous-polymer polystyrene resin Diaion HP-20 (50 mesh, Mitsubishi Chemical, Tokyo, Japan), Si gel Chromatorex BW-300 (300 mesh, Fuji-Silysia Chemical, Aichi, Japan), and COSMOSIL 75C_{18}-OPN (75 μM particle size, Nacalai Tesque, Kyoto, Japan) were used for column chromatography (CC). TLC was performed on precoated Si gel 60 F_{254} or RP_{18} F_{254S} plates (0.25 mm thick, Merck), and spots were visualized by spraying the plates with 10% H_2SO_4 aqueous solution and heating. HPLC separation was performed with a system consisting of an LC-20AD pump (Shimadzu, Kyoto, Japan), a RID-10A refractive index detector (Shimadzu), and a Rheodyne

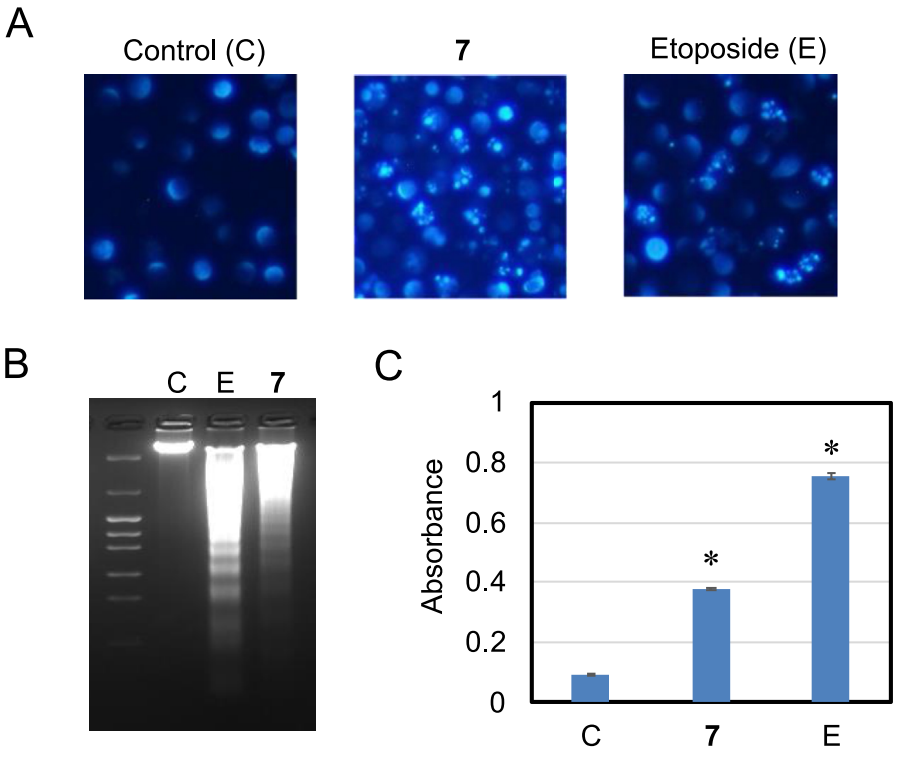

Fig. 4. Compound **7** induced apoptosis in HL-60 cells.
A, Morphology of HL-60 cells treated with **7**. HL-60 cells were stained with DAPI after treatment with either 0.21 μM of **7** or 15 μM of etoposide for 15 h and then observed under a fluorescence microscope. B, Electrophoretic profile of the DNA of HL-60 cells treated with **7**. HL-60 cells were incubated with either 0.21 μM of **7** or 15 μM of etoposide for 15 h. DNA was then extracted and analyzed by agarose gel electrophoresis. C, Caspase-3 activity in the lysates of HL-60 cells treated with **7**. HL-60 cells were incubated with either 0.21 μM of **7** or 15 μM of etoposide for 12 h, and the caspase-3 activity in the lysates was measured using a caspase-3 colorimetric kit. The data are presented as the mean ± S.E.M. of three experiments. Results significantly different from that of the control group are indicated by * ($p < 0.001$).

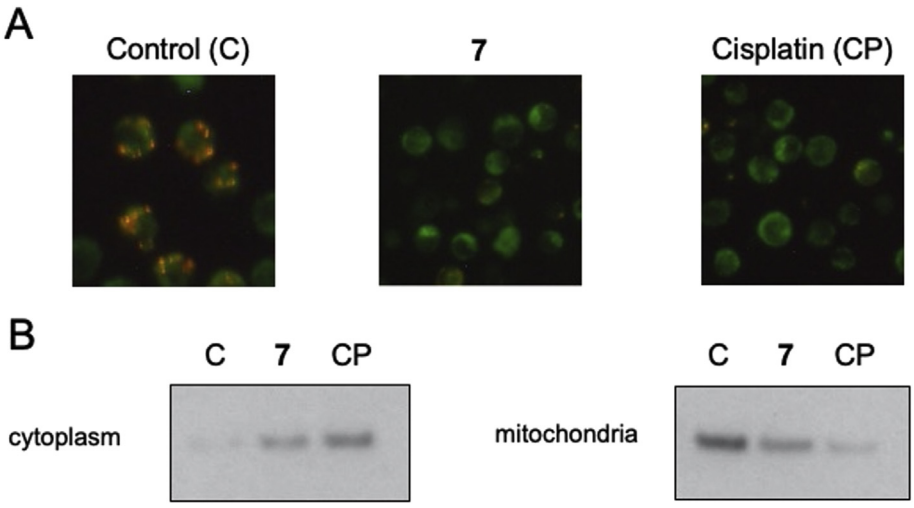

Fig. 5. Compound **7** induced apoptosis through a mitochondria-dependent pathway.
A, Mitochondrial membrane morphology of HL-60 cells treated with **7**. HL-60 cells were stained with MitoCapture™ reagent after treatment with either 0.21 μM of **7** or 33 μM of cisplatin for 6 h and observed under a fluorescence microscope. B, Release of cytochrome *c* from mitochondria of HL-60 cells treated with **7**. HL-60 cells were treated with either 0.21 μM of **7** or 33 μM of cisplatin for 8 h, and the release of cytochrome *c* into the cytoplasm was evaluated by Western blot analysis.

Table 4
Na^+/K^+ ATPase inhibitory activity of **1–10** and ouabain.[a]

Compounds	IC_{50} (μM)
1	0.140 ± 0.007
2	0.100 ± 0.014
3	0.087 ± 0.003
4	0.086 ± 0.002
5	0.450 ± 0.019
6	0.540 ± 0.003
7	0.037 ± 0.001
8	0.049 ± 0.003
9	0.061 ± 0.002
10	0.023 ± 0.002
ouabain	0.110 ± 0.002

[a] Data are presented as the mean value ± S.E.M. of three experiments perfomed in triplicate.

injection port (Rheodyne LLC, Rohnert Park, CA, USA). A TSK gel ODS-100Z column (10 mm i.d. × 250 mm, 5 μm, Tosoh, Tokyo, Japan) was used for preparative HPLC. HL-60 cells (JCRB0085), A549 cells (JCRB0076), and TIG-3 cells (JCRB0510) were obtained from the Japanese Collection of Research Bioresources (JCRB) cell bank (Osaka, Japan). The following materials and reagents were used for the cell culture assays: SH-1300 microplate reader (Corona Electric, Ibaraki, Japan); 96-well flat-bottom plates (Iwaki Glass, Chiba, Japan); fetal bovine serum (FBS), 0.25% trypsin-EDTA solution, RPMI 1640 medium, Dulbecco's Modified Eagle's Medium (DMEM), etoposide, cisplatin, and 3-(4,5-dimethylthiazol-2-yl)-2,5-diphenyl-2*H*-tetrazolium bromide (MTT), naringinase (EC 3.2.1.40) (Sigma-Aldrich, MO, USA); penicillin G sodium salt, streptomycin sulfate, and phosphate buffered saline (PBS) (Wako Pure Chemical Industries, Osaka, Japan). All other chemicals used were of biochemical reagent grade.

4.2. Plant material

The whole plants of *Helleborus lividus* Aiton ex Curtis (Ranunculaceae) were purchased from Fuji Green Co., Ltd (Tokyo, Japan) in June 2007 and the identity was confirmed by one of the authors, A. Yokosuka. A voucher specimen has been deposited in our laboratory (voucher No. KS-2007-001, Department of Medicinal Pharmacognosy).

4.3. Extraction and isolation

The plant material (fresh weight, 4.85 kg) was extracted with hot MeOH (53 L). The MeOH extract (305 g), which showed cytotoxicity against HL-60 cells with an IC_{50} value of 1.3 μg/mL, was loaded on a Diaion HP-20 CC, and successively eluted 30% aqueous MeOH, 50% aqueous MeOH, 100% MeOH, EtOH, and EtOAc. The 50% aqueous MeOH and 100% MeOH eluted portions were cytotoxic to HL-60 cells with 0.15 μg/mL and 0.16 μg/mL, respectively. The 50% aqueous MeOH eluted fraction (12 g) was subjected to Si gel CC and eluted with a stepwise gradient mixture of EtOAc-MeOH-H_2O (190:10:1; 90:10:1; 40:10:1) to produce 17 fractions (A-Q). Fraction G was purified by Si gel CC eluted with hexane-Me_2CO (1:1; 2:3; and 1:2), and ODS Si gel CC eluted with CH_3CN–H_2O (2:7) and MeOH–H_2O (2:3) to give **8** (33.8 mg). Fraction H was purified by Si gel CC eluted with hexane-Me_2CO (2:3 and 1:3), and ODS Si gel CC eluted with CH_3CN–H_2O (1:4) to give **7** (8.4 mg). Fraction L was purified by ODS Si gel CC eluted with MeOH–H_2O (1:4; 1:3; and 1:2) and MeCN–H_2O (1:5), and Si gel CC eluted with hexane-Me_2CO (2:3 and 1:3) to give **2** (14.4 mg) and **4** (2.8 mg). Fraction M was purified by ODS Si gel CC eluted with MeOH–H_2O (1:3; 1:2; and 2:3), and Si gel CC eluted with EtOAc-MeOH-H_2O (40:10:1) to give **1** (64.3 mg). Fraction N was purified by ODS Si gel CC eluted with MeOH–H_2O (1:3 and 1:2) and CH_3CN–H_2O (1:4), and Si gel CC eluted with hexane-Me_2CO (1:4) to give **6** (3.8 mg) and **9** (8.5 mg). Fraction O was purified by ODS Si gel CC eluted with MeOH–H_2O (1:2), and Si gel CC eluted with EtOAc-MeOH-H_2O (20:10:1) to give **3** (15.1 mg). The 100% MeOH eluted fraction (22 g) was subjected to Si gel CC eluted with a stepwise gradient mixture of $CHCl_3$–MeOH–H_2O (90:10:1; 40:10:1; and 20:10:1) to produce 10 fractions (a–j). Fraction c was purified by ODS Si gel CC eluted with MeCN–H_2O (1:3) and MeOH–H_2O (9:11), Si gel CC eluted with $CHCl_3$–MeOH–H_2O (170:30:1), and preparative HPLC using MeCN–H_2O (1:3) as the mobile phase to give **10** (3.0 mg). Fraction d was purified by ODS Si gel CC eluted with MeCN–H_2O (3:7) and MeOH–H_2O (11:9), Si gel CC eluted with $CHCl_3$–MeOH–H_2O (170:30:1), and preparative HPLC using MeCN–H_2O (3:7) as the mobile phase to give **5** (10.7 mg).

4.3.1. 3β-[(β-D-Glucopyranosyl)oxy]-14β,16β-dihydroxy-19-oxo-5α-bufa-20,22-dienolide (1)

Amorphous solid; $[\alpha]_D^{25}$ 4.2 (MeOH; *c* 0.10); UV λ_{max} (MeOH) nm (log ε): 295 (3.71), 204 (4.02); IR ν_{max} (film) cm^{-1}: 3397 (OH), 2922 (CH), 1706 and 1695 (C=O); ^1H NMR (500 MHz, CD_3OD): see Table 1; ^{13}C NMR (125 MHz, CD_3OD): see Table 2; HRESITOFMS *m/z*: 601.2620 $[M + Na]^+$ (calcd for $C_{30}H_{42}O_{11}Na$, 601.2625).

4.3.2. Enzymatic hydrolysis of 1, 3, and 7

Compounds **1** (10 mg), **3** (2.0 mg), and **7** (2.4 mg) were independently treated with naringinase (20 mg for **1**; 4.0 mg for **3**; 5.9 mg for **7**) in AcOH/AcOK buffer (pH 4.3, 2.0 mL) at room temperature for 72 h. The crude hydrolysates were chromatographed on Si gel and

eluted with $CHCl_3$–MeOH–H_2O (90:10:1) to yield **1a** (4.0 mg from **1**; 0.84 mg from **3**; 0.93 mg from **7**) and sugar fractions (3.6 mg from **1**; 0.56 mg from **3**; 0.97 mg from **7**). All the sugar fractions of **1**, **3**, and **7** were analyzed using HPLC under following conditions: column: Capcell Pak NH2 UG80 (4.6 mm i.d. × 250 mm, 5 μm, Shiseido, Tokyo, Japan); solvent: MeCN–H_2O (17:3); detection: optical rotation (OR); flow rate: 0.8 mL/min. HPLC analyses of the sugar fractions showed the presence of D-glucose in those of **1** and **3**, and of L-rhamnose and D-glucose in that of **7**. t_R (min): 10.2 (L-rhamnose, negative optical rotation) and 14.5 (D-glucose, positive optical rotation).

4.3.3. 16β-Acetoxy-3β-[(β-D-glucopyranosyl)oxy]-14β-hydroxy-19-oxo-5α-bufa-20,22-dienolide (2)

Amorphous solid; $[\alpha]_D^{25}$ 1.7 ($CHCl_3$–MeOH, 1:1; *c* 0.10); UV λ_{max} (MeOH) nm (log ε): 295 (3.62), 204 (3.91); IR ν_{max} (film) cm^{-1}: 3397 (OH), 2922 (CH), 1714 and 1697 (C=O); ^1H NMR (600 MHz, CD_3OD): see Table 1; ^{13}C NMR (150 MHz, CD_3OD): see Table 2; HRESITOFMS *m/z*: 621.2917 $[M + Na]^+$ (calcd for $C_{32}H_{44}O_{12}Na$, 621.2911).

4.3.4. Conversion of 2 to 1

A solution of **2** (2.0 mg) was treated with 0.5% NaOMe in MeOH (1.0 mL) at room temperature for 5 min. The reaction mixture was neutralized by passage through an Amberrite IR-120B (Organo, Tokyo, Japan) and chromatographed on Si gel eluted with $CHCl_3$–MeOH–H_2O (90:10:1) to give **1** (0.60 mg).

4.3.5. 3β-[(O-β-D-Glucopyranosyl-(1 → 4)- β-D-glucopyranosyl)oxy]-14β,16β-dihydroxy-19-oxo-5α-bufa-20,22-dienolide (3)

Amorphous solid; $[\alpha]_D^{25}$ –2.5 (MeOH; *c* 0.10); UV λ_{max} (MeOH) nm (log ε): 293 (3.78), 204 (4.13); IR ν_{max} (film) cm^{-1}: 3388 (OH), 2921 (CH), 1708 and 1659 (C=O); ^1H NMR (600 MHz, CD_3OD): see Table 1; ^{13}C NMR (150 MHz, CD_3OD): see Table 2; HRESITOFMS *m/z*: 763.3156 $[M + Na]^+$ (calcd for $C_{36}H_{52}O_{16}Na$, 763.3153).

4.3.6. 3β,5β,14β,16β,19-Pentahydroxybufa-20,22-dienolide (4)

Amorphous solid; $[\alpha]_D^{25}$ 19.5 (MeOH; *c* 0.10); UV λ_{max} (MeOH) nm (log ε): 296 (3.45), 204 (3.66); IR ν_{max} (film) cm^{-1}: 3383 (OH), 2936 (CH), 1702 (C=O); ^1H NMR (600 MHz, CD_3OD): see Table 1; ^{13}C NMR (150 MHz, CD_3OD): see Table 2; HRESITOFMS *m/z*: 457.2202 $[M + Na]^+$ (calcd for $C_{24}H_{34}O_7Na$, 457.2202).

4.3.7. 1β,3β,5β,14β,16β-Pentahydroxybufa-20,22-dienolide (5)

Amorphous solid; $[\alpha]_D^{25}$ 16.9 (MeOH; *c* 0.08); UV λ_{max} (MeOH) nm (log ε): 294 (2.99), 205 (3.33); IR ν_{max} (film) cm^{-1}: 3385 (OH), 2924 (CH), 1704 (C=O); ^1H NMR (500 MHz, CD_3OD): see Table 1; ^{13}C NMR (125 MHz, CD_3OD): see Table 2; HRESITOFMS *m/z*: 457.2201 $[M + Na]^+$ (calcd for $C_{24}H_{34}O_7Na$, 457.2202).

4.3.8. 5β,14β,16β-Trihydroxy-3β-[(α-L-rhamnopyranosyl)oxy]-bufa-20,22-dienolide (6)

Amorphous solid; $[\alpha]_D^{25}$ 2.2 (MeOH; *c* 0.05); UV λ_{max} (MeOH) nm (log ε): 295 (2.73), 206 (3.75); IR ν_{max} (film) cm^{-1}: 3388 (OH), 2925 (CH), 1704 (C=O); ^1H NMR (600 MHz, CD_3OD): see Table 1; ^{13}C NMR (150 MHz, CD_3OD): see Table 2; HRESITOFMS *m/z*: 587.2834 $[M + Na]^+$ (calcd for $C_{30}H_{44}O_{10}Na$, 587.2832).

4.3.9. Acid hydrolysis of 6

Compound **6** (1.2 mg) was treated with 1 M HCl in dioxane-H_2O (1:1, 2.0 mL) at 95 °C for 1 h. The crude hydrolysate was neutralized by passage through an Amberlite IRA-96SB (Organo) column and subjected to a Diaion HP-20 column eluted with MeOH–H_2O (3:2) followed by EtOH–Me_2CO (1:1) to yield the sugar fractions (0.18 mg). HPLC analysis of the sugar fraction under the same conditions used for **1**, **3**, and **7** showed the presence of L-rhamnose. t_R (min): 10.2 (L-rhamnose, negative optical rotation).

4.3.10. 3β-[(O-β-D-Glucopyranosyl-(1 → 4)-α-L-rhamnopyranosyl)oxy]-14β,16β-dihydroxy-5β-bufa-20,22-dienolide (7)

Amorphous solid; $[\alpha]_D^{25}$ –18.1 (MeOH; *c* 0.05); UV λ_{max} (MeOH) nm (log ε): 295 (3.70), 206 (3.81); IR ν_{max} (film) cm^{-1}: 3376 (OH), 2934 (CH), 1728 (C=O); ^1H NMR (500 MHz, CD_3OD): see Table 1; ^{13}C NMR (125 MHz, CD_3OD): see Table 2; HRESITOFMS *m/z*: 733.3417 $[M + Na]^+$ (calcd for $C_{36}H_{54}O_{14}Na$, 733.3411).

4.4. Assay for cytotoxic activity

The cytotoxic activity of the test compounds against HL-60 and A549 tumor cells and TIG-3 normal cells was established using an MTT reduction assay, as previously described (Yokosuka et al., 2018).

4.5. Assay for Na^+/K^+ ATPase inhibitory activity

The Na^+/K^+ ATPase inhibitory activity of the test compounds was performed as previously described (Iguchi et al., 2020).

4.6. Assay for apoptosis inducing activity

The morphological observations with DAPI staining, the detection of DNA fragmentation, activation of caspase-3, disruption of mitochondrial membrane potential ($\Delta\Psi m$), and release of cytochrome *c* into the cytosol were performed as previously described (Yokosuka et al., 2018).

4.7. Statistical analysis

For statistical analysis, one-way analysis of variance (ANOVA) followed by Dunnett's test was performed. A probability (*p*) value of less than 0.001 was considered to represent a statistically significant difference.

Declaration of competing interest

The authors declare no conflict of interest associated with this manuscript.

Acknowledgements

This work was financially supported in part by the Japan Society for the Promotion of Science (JSPS) KAKENHI Grant Numbers JP26860069 and JP18K06735.

Appendix A. Supplementary data

Supplementary data to this article can be found online at https://doi.org/10.1016/j.phytochem.2020.112415.

References

Bock, K., Lundt, I., Pedersen, C., 1973. Assignment of anomeric structure to carbohydrates through geminal ^{13}C-H coupling constants. Tetrahedron Lett. 14, 1037–1040.
Cheng, W., Tan, Y.F., Tian, H.Y., Gong, X.W., Chen, K.L., Jiang, R.W., 2014. Two new bufadienolides from the rhizomes of *Helleborus thibetanus* with inhibitory activities against prostate cancer cells. Nat. Prod. Res. 28, 901–908.
Iguchi, T., Yokosuka, A., Kawahata, R., Audou, M., Mimaki, Y., 2020. Bufadienolides from the whole plants of *Helleborus foetidus* and their cytotoxicity. Phytochemistry 172, 112277.
Krenn, L., Jelovina, M., Kopp, B., 2000. New bufadienolides from *Urginea maritima sensu strictu*. Fitoterapia 71, 126–129.
Meng, Y., Whiting, P., Sik, V., Rees, H.H., Dinan, L., 2001. Ecdysteroids and bufadienolides from *Helleborus torquatus* (Ranunculaceae). Phytochemistry 57, 401–407.
Tsukamoto, Y. (Ed.), 1989. The Grand Dictionary of Horticulture, vol. 4. Shogakukan, Tokyo, pp. 387–389.
Van Wyk, A.J., Enslin, P.R., 1968. Bufadienolides of *Moraea polystachya* and *M. graminicola*. J. South African Chem. Inst. 21, 33–38.
Verpoorte, R., Kinh, P.Q., Svendsen, B., 1980. Chemical constituents of Vietnamese toad

venom, collected from *Bufo melanostictus* Schneider. part II. The bufadienolides. J. Nat. Prod. 43, 347–352.
Watanabe, K., Mimaki, Y., Sakagami, H., Sashida, Y., 2003. Bufadienolide and spirostanol glycosides from the rhizomes of *Helleborus orientalis*. J. Nat. Prod. 66, 236–241.
Yokosuka, A., Iguchi, T., Kawahata, R., Mimaki, Y., 2018. Cytotoxic bufadienolides from the whole plants of *Helleborus foetidus*. Phytochem. Lett. 23, 94–99.
Zeino, M., Brenk, R., Gruber, L., Zehl, M., Urban, E., Kopp, B., Efferth, T.J., 2015. Cytotoxicity of cardiotonic steroids in sensitive and multidrug-resistant leukemia cells and the link with Na^+/K^+-ATPase. Steroid Biochem. Mol. Biol. 150, 97–111.
Zhang, H., Su, Y., Yang, F., Zhao, Z., Gao, X., 2014. Two new bufadienolides and one new pregnane from *Helleborus thibetanus*. Phytochem. Lett. 10, 164–167.